EPJ Web of Conferences **172**, 05003 (2018) https://doi.org/10.1051/epjconf/201817205003
ISMD 2017

Recent ATLAS measurements of azimuthal anisotropies in pp and p+Pb collisions

Adam Trzupek[1,⋆] on behalf of the ATLAS Collaboration

[1] *Institute of Nuclear Physics PAS, ul. Radzikowskiego 152, 31-342 Kraków, Poland*

Abstract. The azimuthal anisotropies of particle yields observed in relativistic heavy-ion collisions are considered as an evidence of the formation on a deconfined Quark-Gluon Plasma produced in these collisions. Interestingly, recent measurements in pp and p+Pb systems from ATLAS and other experiments show similar features as those observed in A+A collisions, indicating the possibility of the production of such a deconfined medium in smaller collision systems. This report presents a summary of the recent ATLAS results on azimuthal anisotropies in pp collisions at 5.02 TeV and 13 TeV, p+Pb collisions at 5.02 TeV and 8.16 TeV as well as in peripheral 2.76 TeV Pb+Pb interactions. It includes measurements of two-particle correlations of charged particles as well as correlations of heavy flavor muons and charged particles in $\Delta\phi$ and $\Delta\eta$, with a template fitting procedure used to subtract the dijet contributions. Additionally, measurements of cumulants of multi-particle correlations, $c_n\{2\text{–}8\}$ are presented. The two-particle correlations and cumulants confirm a presence of collective phenomena in these collision systems, but the results on four-particle cumulants for pp collisions do not demonstrate a similar collective behaviour. However, the cumulant measurements in small collision systems can be biased by non-flow correlations. A novel subevent cumulant method that suppresses the contribution of non-flow effects was proposed recently by ATLAS allowing to measure significant azimuthal anisotropies in both pp and p+Pb collisions.

ATL-PHYS-PROC-2017-226
23 October 2017

1 Introduction

One of the main signatures of the formation of strongly interacting Quark-Gluon Plasma (QGP) in heavy-ion collisions at the Relativistic Heavy Ion Collider (RHIC) and the Large Hadron Collider (LHC) is the large azimuthal anisotropy of produced particles [1, 2]. Interestingly, significant azimuthal anisotropy was also observed (at the LHC for the first time) in pp and p+Pb collisions [3, 4]. Since the first measurements, the collective phenomena in small systems are under extensive theoretical and experimental study, which significantly improves our understanding of the flow phenomena in heavy-ion collisions. However, there are still open questions such as what is the underlying mechanism for the observed correlations, what is the role of initial effects or whether the QGP exists in collisions involving light nuclei. In this report, the recent ATLAS [5] results on Fourier coefficients v_n of charged-particle azimuthal distributions, extracted from the two-particle correlations using a novel template fitting method, are shown for pp collisions at $\sqrt{s}$ = 5.02 TeV and 13 TeV and p+Pb collisions at $\sqrt{s_{\rm NN}}$ = 5.02 TeV [6] and $\sqrt{s_{\rm NN}}$ = 8.16 TeV [7]. The template fitting method was also used

⋆e-mail: adam.trzupek@ifj.edu.pl

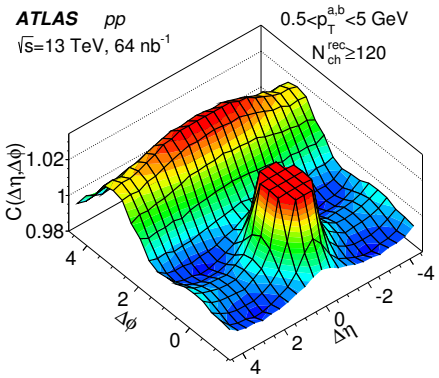

Figure 1. Two-particle correlation functions $C(\Delta\eta, \Delta\phi)$ in 13 TeV pp collisions corresponding to multiplicity range of $N_{\rm ch}^{\rm rec}$ ≥120. The plots are for charged particles of $0.5 < p_{\rm T}^{a,b} < 5$ GeV. The distribution has been truncated to suppress the peak at $\Delta\eta = \Delta\phi = 0$ [4].

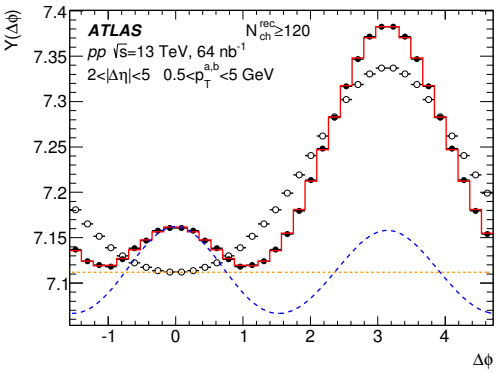

Figure 2. Template fits to the per-trigger particle yields $Y(\Delta\phi)$, in 13 TeV pp collisions for high multiplicity events of $N_{\rm ch}^{\rm rec}$ ≥120. The solid points indicate the measured $Y(\Delta\phi)$, the open points and curves show different components of the template fit [4].

to obtain v_2 of muons from heavy-flavor hadron decays in p+Pb collisions at $\sqrt{s_{\rm NN}}$ = 8.16 TeV [7]. For the small collision systems and additionally for low-multiplicity $\sqrt{s_{\rm NN}}$ = 2.76 TeV Pb+Pb collisions, the measurements of multi-particle cumulants and corresponding flow harmonics are also presented [8, 9].

2 Two-particle correlations

The two-particle correlation technique [3, 4] is deployed to measure the azimuthal anisotropy in small systems and is also commonly applied to probe collective phenomena in heavy-ion collisions [10–12]. Recently, a two-particle correlation analysis was performed by ATLAS [6, 7, 13] for pp collisions at $\sqrt{s}$ = 2.76 TeV, 5.02 TeV and 13 TeV, and for p+Pb collisions at $\sqrt{s_{\rm NN}}$ = 5.02 TeV and 8.16 TeV. For low-multiplicity pp or p+Pb collisions, the correlation function measured in the relative pseudorapidity ($\Delta\eta$) and azimuthal angle ($\Delta\phi$) of two charged particles with transverse momenta $p_{\rm T}^a$ and $p_{\rm T}^b$, is dominated by non-flow effects due to jet production, momentum conservation, resonance decays or Bose-Einstein correlations. The correlation function features a sharp peak centered at $(\Delta\phi, \Delta\eta) = (0, 0)$ and a broad, extended in $\Delta\eta$ structure at $\Delta\phi \approx \pi$. In high-multiplicity collisions, see Figure 1, an additional long-range structure in $\Delta\eta$ at $\Delta\phi \approx 0$, called "near-side ridge", is clearly visible. Also the correlation function at $\Delta\phi \approx \pi$ is broadened relative to low-multiplicity collisions, revealing a presence of the "away-side ridge". The strength of the ridge correlations is commonly quantified by the "per-trigger yield", $Y(\Delta\phi)$, which measures the average number of particle pairs associated with a trigger particle with $p_{\rm T}^a$ at the large pseudorapidity separation, $|\Delta\eta| > 2$, imposed to suppress the non-flow correlations. Using a template fitting function, the per-trigger yield is separated into two components: a scaled per-trigger yield for low-multiplicity interactions, $Y^{\rm periph}(\Delta\phi)$, describing the back-to-back jet correlations, and an azimuthal modulation term describing the ridge, see Figure 2. In this approach, the non-flow correlations are described by the fit function, therefore, there is no need to perform the "peripheral subtraction" procedure on $Y(\Delta\phi)$ or $Y^{\rm periph}(\Delta\phi)$, which has been commonly used in other analyses. In the peripheral subtraction procedure the non-flow effects are suppressed by setting the Y pedestal level by a zero-yield at minimum (ZYAM) [6]. The azimuthal modulation

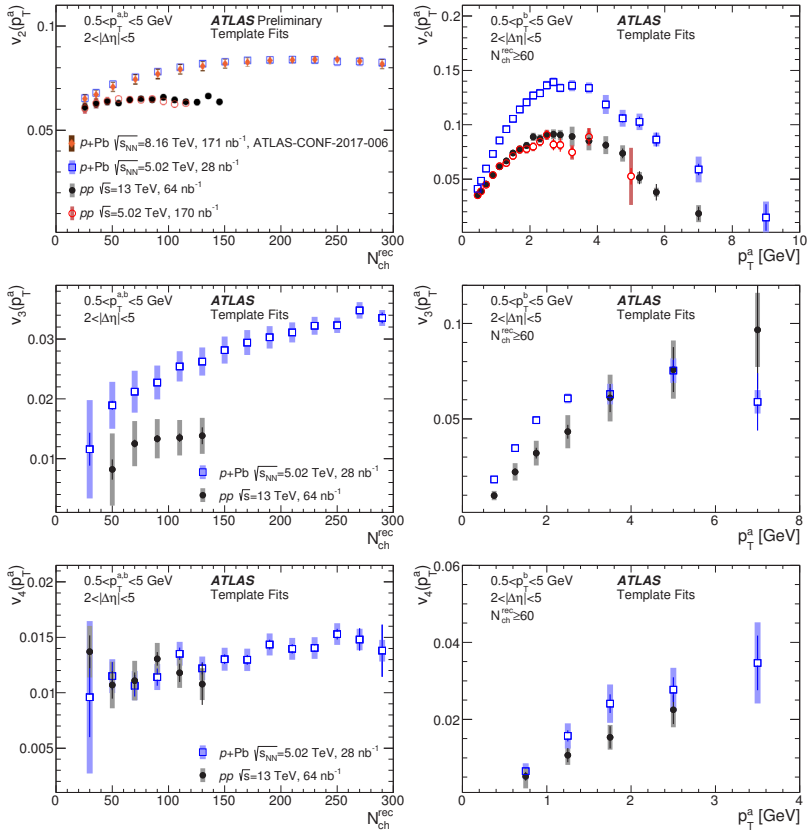

Figure 3. The $N_{\mathrm{ch}}^{\mathrm{rec}}$- and p_{T}-dependences of the v_n in 13 TeV pp, 5.02 TeV pp, 5.02 TeV p+Pb and 8.16 TeV p+Pb collisions. Panels from top to bottom correspond to n=2, 3 and 4 respectively. The plots are for charged particles forming a pair with $0.5 < p_{\mathrm{T}} < 5$ GeV [6, 7].

amplitudes $2v_{n,n}$ obtained from the fitting procedure were found to factorize into a product of single particle flow harmonics $v_n \cdot v_n$, hence the flow harmonics are obtained from the formula: $v_n = \sqrt{v_{n,n}}$. A weak variation of $v_{n,n}$ on the applied pseudorapidity $|\Delta\eta|$ cut was observed. Figure 3 (the left column) shows measurements of v_2, v_3 and v_4 harmonics in 5.02 TeV and 13 TeV pp, and 5.02 TeV and 8.16 TeV p+Pb collisions as a function of the number of charged particles with $p_{\mathrm{T}} > 0.4$ GeV and $|\eta| < 2.5$, $N_{\mathrm{ch}}^{\mathrm{rec}}$. One can see that all three v_n harmonics in 5.02 TeV and 13 TeV pp data are $N_{\mathrm{ch}}^{\mathrm{rec}}$-independent, while the p+Pb v_2, v_3 and v_4 increase with increasing event multiplicity, except for v_2, which starts to be multiplicity independent for $N_{\mathrm{ch}}^{\mathrm{rec}} > 150$. Figure 3 also shows a comparison of the v_2 harmonic measured in p+Pb at $\sqrt{s_{\mathrm{NN}}} = 8.16$ TeV to those measured at $\sqrt{s_{\mathrm{NN}}} = 5.02$ TeV. The v_2 harmonics at the two collision energies are consistent within the systematic uncertainties.

Figure 3 (the right column) shows the p_{T} dependence of v_n in 5.02 and 13 TeV pp, and 5.02 TeV p+Pb collisions for $N_{\mathrm{ch}}^{\mathrm{rec}} \geq 60$. Similar v_2 harmonics are observed in pp collisions at both collision energies. With increasing transverse momentum, v_2 harmonics rise reaching a maximum near 3 GeV and then drop, reaching almost 0 at $p_{\mathrm{T}} \approx 7$ GeV. A more rapid increase of v_2 is observed in p+Pb collisions, but generally a similar trend is preserved in both systems. The v_3 harmonics in 13 TeV pp collisions increase with increasing p_{T} over the measured transverse momentum range. For p+Pb

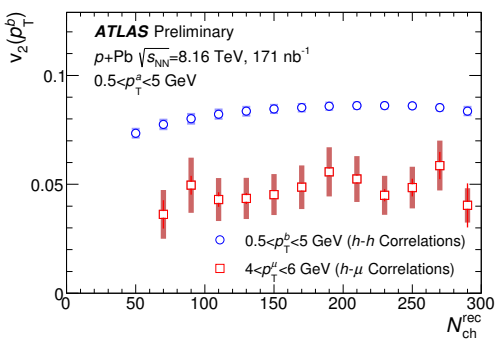

Figure 4. The v_2 values obtained from the template fits to $h-h$ correlations with $0.5 < p_{\mathrm{T}}^{a,b} < 5$ GeV (circles) and to $h-\mu$ correlations with $4 < p_{\mathrm{T}}^{\mu} < 6$ GeV (squares) [4].

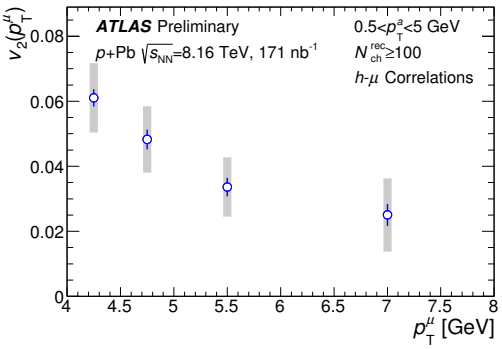

Figure 5. The p_T dependence of the muon-v_2 integrated over a broad multiplicity range of $N_{\mathrm{ch}}^{\mathrm{rec}} \geq 100$ [4].

collisions, larger v_3 values are measured than in pp for $p_{\mathrm{T}} < 3$ GeV. At higher p_{T}, v_3 in p+Pb data saturates. The v_4 harmonics in 13 TeV pp and 5.02 TeV p+Pb collisions increase with increasing transverse momentum and larger v_4 values are measured in p+Pb than in pp collisions.

3 Correlations between muons and charged-particles

Charm and bottom quarks provide an important signature of the QGP formed in ultra-relativistic heavy ion collisions [14]. It is expected that at high transverse momenta, $p_{\mathrm{T}} \gg 5$ GeV, heavy quarks produced in the early stage of the collision lose energy in the QGP with mass-dependent modifications [15]. At lower transverse momenta, $p_{\mathrm{T}} \lesssim 5$ GeV, the quarks are expected to interact with the hot and dense medium acquiring an azimuthal anisotropy due to the collective expansion of the QGP. Measurements of heavy flavor quarks in A+A collisions were performed at RHIC and LHC [16–18]. A significant suppression of heavy quarks production due to energy loss was observed as well as a significant azimuthal anisotropy was measured.

Recently, ATLAS performed a measurement of the long-range correlations between reconstructed muons of $4 < p_{\mathrm{T}}^{\mu} < 8$ GeV and inclusive charged particles in p+Pb collisions at $\sqrt{s} = 8.16$ TeV [7]. Majority of prompt muons at low transverse momenta, $p_{\mathrm{T}} \lesssim 5$ GeV, results from decays of heavy-flavor hadrons containing charm or bottom quarks [19]. Therefore, if a QGP is formed in p+Pb collisions, its collective expansion may influence heavy-flavor hadron production [20], which can be probed by the measurement of two-particle correlations.

Based on a Monte Carlo simulation of the ATLAS detector [7], it was found that the sample of reconstructed muons with $4 < p_{\mathrm{T}} < 8$ GeV is contaminated up to 45% by background muons originating from pion and kaon decays, muons produced in hadronic showers, and mis-associations of Inner Detector (ID) and Muon Spectrometer (MS) tracks. To lower the background fractions, the momentum imbalance, $\Delta p/p_{ID} = (p_{ID} - p_{MS})/p_{ID}$, is calculated for each muon, where p_{ID} and p_{MS} are the reconstructed muon momenta measured in the ID and MS, respectively. As the momentum of background muons measured in the MS is typically lower than the momentum measured in the ID, majority of background muons are characterised by the positive momentum imbalance, $\Delta p/p_{ID} > 0$. Therefore, only muons with $\Delta p/p_{ID} < 0$ are accepted for the correlation measurement. This require-

ment lowers the background fractions to 25% – 10% for the muon transverse momentum range from 4 GeV to 8 GeV.

The two-particle correlations of reconstructed muons and charged particles ($h-\mu$), obtained in a similar way as the two-particle correlations for inclusive charged particles ($h-h$), show a clear ridge structure in the high-multiplicity 8.16 TeV p+Pb collisions. To extract the muon-v_2, the two-particle correlation template fitting method, described in Section 2, is used. Figure 4 shows the measured muon-v_2 obtained from $h-\mu$ correlations of $4 < p_{\mathrm{T}}^{\mu} < 6$ GeV and $0.5 < p_{\mathrm{T}}^{a} < 5$ GeV as well as charged-particle v_2 obtained from $h-h$ correlations of $0.5 < p_{\mathrm{T}}^{a,b} < 5$ GeV. Within systematic uncertainties, the muon-v_2 remains constant over the measured $N_{\mathrm{ch}}^{\mathrm{rec}}$ range, and is smaller than v_2 for charged particles. However, it should be noted that different p_{T} ranges are used for both measurements. Figure 5 shows the p_{T} dependence of the muon-v_2 over transverse momentum range $4 < p_{\mathrm{T}}^{\mu} < 8$ GeV measured for large multiplicity events of $N_{\mathrm{ch}}^{\mathrm{rec}} \geq 100$. A decrease of muon-$v_2$ is observed with increasing p_{T}^{μ}.

4 Multi-particle cumulants

A commonly used approach to measure flow harmonics, which efficiently suppresses the non-flow correlations, is the multi-particle cumulant method [21, 22]. In this method, the $2k$-particle azimuthal correlations, $corr_n\{2k\}$, are calculated and then used to obtain the multi-particle cumulants, $c_n\{2k\}$. By definition, $2k$-particle cumulants describe genuine $2k$-particle correlations, i.e. the correlations between fewer number of particles than $2k$, which include most of non-flow correlations, are subtracted. The cumulant method was used for systems including Pb+Pb, p+Pb and recently pp collisions [23–26]. ATLAS measured multi-particle cumulants in pp collisions at $\sqrt{s} = 5.02$ TeV and 13 TeV, and $\sqrt{s_{\mathrm{NN}}} = 5.02$ TeV p+Pb and in low-multiplicity Pb+Pb collisions at $\sqrt{s_{\mathrm{NN}}} = 2.76$ TeV [8]. To avoid event multiplicity fluctuations, which can mimic the collective-like effects [8, 24], cumulants are calculated in unit-size bins in the number of reference particles, M_{ref}, which is defined as the number of reconstructed charged particles with $|\eta| < 2.5$ and with p_{T} range: $0.3 < p_{\mathrm{T}} < 3$ GeV or $0.5 < p_{\mathrm{T}} < 5$ GeV. The cumulants are then calculated in broader, statistically significant multiplicity intervals by

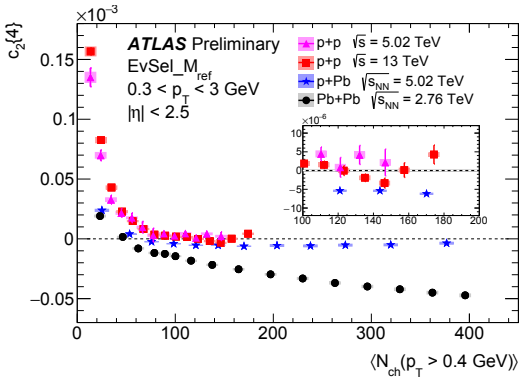

Figure 6. The second order cumulant $c_2\{4\}$ obtained from four-particle correlations as a function of $\langle N_{\mathrm{ch}}(p_{\mathrm{T}} > 0.4\ \mathrm{GeV})\rangle$ for pp collisions at $\sqrt{s} = 5.02$ and 13 TeV, p+Pb collisions at $\sqrt{s_{\mathrm{NN}}} = 5.02$ TeV and Pb+Pb collisions at $\sqrt{s_{\mathrm{NN}}} = 2.76$ TeV [8].

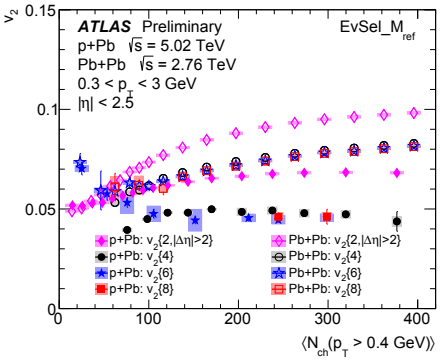

Figure 7. Comparison of $v_2\{2, |\Delta\eta| > 2\}$, $v_2\{4\}$, $v_2\{6\}$ and $v_2\{8\}$ as a function of $\langle N_{\mathrm{ch}}(p_{\mathrm{T}} > 0.4\ \mathrm{GeV})\rangle$ for $\sqrt{s_{\mathrm{NN}}} = 5.02$ TeV p+Pb collisions and $\sqrt{s_{\mathrm{NN}}}$= 2.76 TeV Pb+Pb collisions. The results are presented for particles with $0.3 < p_{\mathrm{T}} < 3$ GeV[8].

averaging with weights corresponding to the total number of $2k$-multiplets in M_{ref} bins and accounting for the event trigger efficiency [8, 22]. Results obtained for different collision systems or p_{T}-ranges

are compared in a common event activity variable, $N_{\rm ch}(p_{\rm T} > 0.4)$, defined as the mean number of charged particles with $p_{\rm T} > 0.4$ GeV in events in the $M_{\rm ref}$ interval used for the cumulant calculations.

Figure 6 shows the four-particle cumulants measurement in pp collisions at $\sqrt{s} = 5.02$ and 13 TeV, p+Pb collisions at $\sqrt{s_{\rm NN}} = 5.02$ TeV and Pb+Pb collisions at $\sqrt{s_{\rm NN}} = 2.76$ TeV for $0.3 < p_{\rm T} < 3$ GeV. One can see that they follow the ordering $|c_2\{4\}|_{\rm p+Pb} < |c_2\{4\}|_{\rm Pb+Pb}$ for $N_{\rm ch}(p_{\rm T} > 0.4$ GeV)>100. Therefore, the magnitude of the corresponding elliptic flow, $v_2\{4\} = \sqrt[4]{-c_2\{4\}}$, is larger for Pb+Pb collisions than for p+Pb events. For 5.02 TeV pp collisions, the $c_2\{4\}$ cumulants are positive or consistent with zero over the full range of particle multiplicities. For the 13 TeV pp data, the cumulants are positive over the large range of multiplicities, with the exception of $N_{\rm ch}$ from 130 to 150, where $c_2\{4\}$ is smaller than zero within 1–2 standard deviations. Therefore, these measurements of positive $c_2\{4\}$ cumulants in pp collisions do not allow to calculate the Fourier harmonics.

Figure 7 shows a comparison of the $v_2\{2, |\Delta\eta| > 2\}$ harmonics calculated with the requirement of pseudorapidity separation $|\Delta\eta| > 2$, $v_2\{4\}$, $v_2\{6\}$ and $v_2\{8\}$, for p+Pb and low-multiplicity Pb+Pb collisions. All derived v_2 harmonics have larger magnitudes in Pb+Pb collisions than in p+Pb collisions with the same multiplicity. For both systems for $N_{\rm ch}$ above 100, $v_2\{2k\}$ are similar for $k = 2$, 3 and 4 while $v_2\{2, |\Delta\eta| > 2\}$ is systematically larger than the harmonics $v_2\{2k\}$ calculated with more than two-particle cumulants due to fluctuations in the initial-state geometry [28].

5 Subevent cumulant method

To further reduce the non-flow correlations, especially in pp collisions and low-multiplicity p+Pb collisions, ATLAS has developed an improved cumulant method based on the correlations between particles from different subevents separated in pseudorapidity [9]. In particular, correlating particles from two subevents constructed of particles with $\eta < 0$ (subevent a) and $\eta > 0$ (subevent b) suppresses non-flow contribution mainly from short-range correlations, like correlations within jets, while in the case of three-subevents correlating particles from subevent b of $|\eta| < 0.833$ with particles from subevents a of $\eta < -0.833$ and c of $\eta > 0.833$, additionally lowers contribution from dijets. The capability of the subevent cumulant method was verified with Pythia 8 event generator [27].

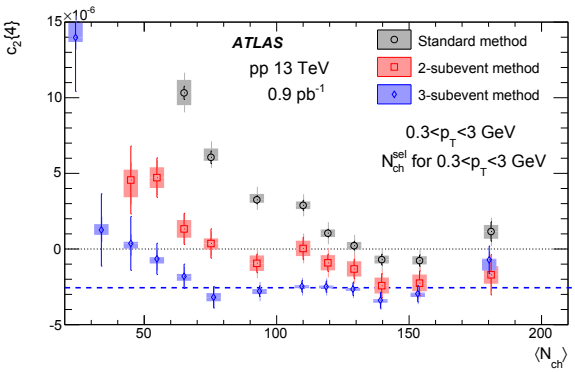

Figure 8. The $c_2\{4\}$ values calculated for charged particles with $0.3 < p_{\rm T} < 3$ GeV compared for the three cumulant methods from the 13 TeV pp data. The event averaging is performed for $N_{\rm ch}^{\rm sel}$ calculated for the same $p_{\rm T}$ range, which is then mapped to $N_{\rm ch}$, the average number of charged particles with $p_{\rm T} > 0.4$ GeV. The dashed line indicates the $c_2\{4\}$ value corresponding to a 4% v_2 signal [9].

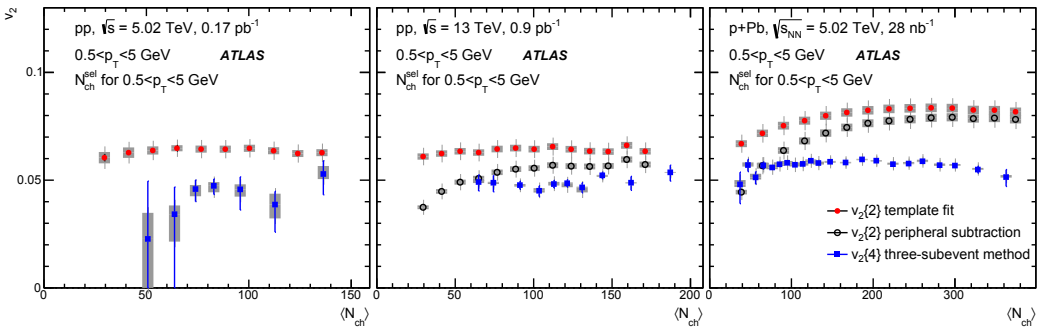

Figure 9. The $v_2\{4\}$ values calculated for charged particles with $0.3 < p_T < 3$ GeV using the three-subevent method in 5.02 TeV pp (left panel), 13 TeV pp (middle panel) and 5.02 TeV p+Pb collisions (right panel). They are compared to v_2 obtained from the two-particle correlation analyses where the non-flow effects are removed by a template fit procedure (solid circles) or with a fit after subtraction with a ZYAM assumption (peripheral subtraction, open circles) [9].

Figure 8 shows a comparison of the four-particle cumulant, $c_2\{4\}$, measured with the standard, two-subevent, and three-subevent methods for pp collisions at $\sqrt{s}$ =13 TeV. A clearly negative value of the $c_2\{4\}$ cumulant obtained with the two- and three-subevent methods is observed for $N_{\rm ch} > 70$, which is consistent with the presence of collectivity in 13 TeV pp collisions. Results for 5.02 TeV pp and low multiplicity ($N_{\rm ch} < 70$) p+Pb collisions at $\sqrt{s_{\rm NN}}$ = 5.02 TeV show similar trends to the results for 13 TeV pp collisions, however, in p+Pb collisions for $N_{\rm ch} > 100$, all three methods give comparable $c_2\{4\}$, suggesting that non-flow effects in p+Pb collisions are much smaller [9].

Negative values of $c_2\{4\}$ obtained from the subevent cumulant methods allow for calculations of flow harmonics. For the three-subevent cumulant method, the $v_2\{4\}$ for reference particles $0.3 < p_T < 3$ GeV in 5.02 TeV pp, 13 TeV pp and 5.02 TeV p+Pb collisions are presented in Figure 9. The results are compared to values of $v_2\{2\}$ obtained from the two-particle correlation template fitting method [10, 15]. For comparison, Figure 9 also shows $v_2\{2\}$ obtained from the two-particle correlation method which sets the pedestal level by a zero-yield at minimum (ZYAM) [6]. The $v_2\{4\}$ values are observed to be approximately independent of $N_{\rm ch}$ and lower than the two-particle correlation results for the three collision systems.

The ratio of the elliptic flow from the four-particle cumulant method and the two-particle correlations allows to estimate the number of independent sources contributing to the particle production, $N_{\rm s}$ [28]. Figure 10 shows the extracted values of $N_{\rm s}$ as a function of $N_{\rm ch}$ in 13 TeV pp and 5.02 p+Pb collisions, for charged particles with $0.3 < p_T < 3$ GeV, using the method presented in Ref. [28]. It is observed that the $N_{\rm s}$ value increases with $N_{\rm ch}$ in p+Pb collisions, reaching $N_{\rm s} \approx 20$ at the highest multiplicity and the $N_{\rm s}$ values for 13 TeV pp and 5.02 TeV p+Pb collisions are similar in the range of overlapping $N_{\rm ch}$ multiplicities.

6 Summary

Using the novel, template fitting two-particle correlation method, v_n (n = 2, 3, 4) harmonics were measured as a function of multiplicity and transverse momentum in pp collisions at $\sqrt{s}$ = 5.02 TeV and 13 TeV as well as in p+Pb collisions at $\sqrt{s_{\rm NN}}$ = 5.02 TeV and 8.16 TeV . The measurement shows that v_2 in pp collisions weakly depends on multiplicity and collision energy. The p+Pb v_2 values are larger than the pp v_2 for all multiplicities and are observed to increase with $N_{\rm ch}^{\rm rec}$. As a

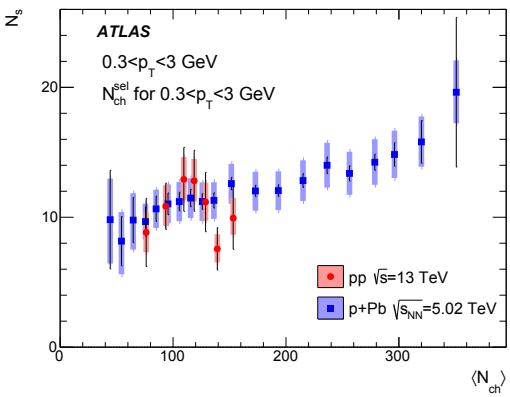

Figure 10. The number of sources inferred from $v_2\{2\}$ and $v_2\{4\}$ measurements via the model framework in 13 TeV pp and 5.02 TeV p+Pb collisions, for charged particles with $0.3 < p_T < 3$ GeV [9].

function of multiplicity, the v_2 harmonics in p+Pb at $\sqrt{s_{NN}} = 5.02$ TeV and 8.16 TeV are consistent within the measurement uncertainty. As a function of p_T, the p+Pb v_2 harmonics are larger than v_2 in pp collisions, but a similar dependence on the transverse momentum is seen, which also resembles the trend observed in Pb+Pb collisions.

The two-particle correlation template fitting method was also used to obtain v_2 of heavy flavor muons of $4 < p_T^{\mu} < 8$ GeV in p+Pb collisions at $\sqrt{s_{NN}} = 8.16$ TeV. The muon-v_2 harmonic is found to be constant as a function of multiplicity, while as a function of the transverse momentum a decrease of muon-v_2 is observed with increasing p_T.

Multi-particle cumulants were measured for pp at $\sqrt{s} = 5.02$ TeV and 13 TeV as well as for p+Pb at $\sqrt{s_{NN}} = 5.02$ TeV collisions and low-multiplicity Pb+Pb collisions at $\sqrt{s_{NN}} = 2.76$ TeV. The collective nature of multi-particle correlations is well confirmed for p+Pb and Pb+Pb collisions for charged-particle multiplicities above 100. The measured v_2 harmonics from multi-particle cumulants have larger values for Pb+Pb collisions as compared to p+Pb collisions and are similar for both systems at $N_{ch} > 100$ for $k = 2$, 3 and 4, while $v_2\{2, |\Delta\eta| > 2\}$ is systematically larger than the $v_2\{2k\}$ calculated with more than two-particle cumulants. This observation is consistent with models assuming fluctuation-driven initial-state anisotropies. For pp collisions, the four-particle cumulants are positive or consistent with zero over the full range of particle multiplicities, with the exception for 13 TeV pp collisions of N_{ch} from 130 to 150, where $c_2\{4\}$ is smaller than zero within 1–2 standard deviations. Therefore, these measurements in pp collisions, do not satisfy the requirement of being negative for the $v_2\{4\}$ harmonic calculation since are biased by non-flow contaminations.

Recently, ATLAS has proposed a novel sub-event method for the $c_2\{4\}$ cumulant measurement, in which particles from different sub-events separated in pseudorapidity are used for cumulant calculations. Monte Carlo simulations show that the subevent cumulant method efficiently suppresses non-flow effects. Clearly negative sign of the four-particle subevent cumulants, $c_2\{4\}$, allow for flow harmonics calculations both in pp and p+Pb collisions. The $v_2\{4\}$ harmonics in pp collisions at $\sqrt{s} =$ 5.02 TeV and 13 TeV and in p+Pb collisions at $\sqrt{s_{NN}} = 5.02$ TeV are observed to be approximately independent of N_{ch} and lower than the two-particle correlation results. These measurements allow studying the fluctuations in the initial-state geometry of small collision systems.

The measurements of two- and multi-particle correlations presented in this report significantly contribute to the understanding of collectivity in small systems and help to constrain the theoretical modelling.

This work was supported in part by the National Science Centre, Poland grant 2016/23/B/ST2/00702 and by PL-Grid Infrastructure.

References

[1] STAR Collaboration, Phys. Rev. Lett. 86 (2001) 402, arXiv: 0009011 [nucl-ex].
[2] ALICE Collaboration, Phys. Rev. Lett. 105 (2010) 252302, arXiv:1011.3914 [nucl-ex].
[3] CMS Collaboration, JHEP 1009 (2010) 091, arXiv:1009.4122 [hep-ex].
[4] ATLAS Collaboration, Phys. Rev. Lett. 110 (2013) 182302, arXiv:1212.5198 [hep-ex].
[5] ATLAS Collaboration, JINST 3 (2008) S08003.
[6] ATLAS Collaboration, PRC 96 (2017) 024908, arXiv:1609.06213 [nucl-ex].
[7] ATLAS Collaboration, ATLAS-CONF-2017-006, url: https://cds.cern.ch/record/2244808.
[8] ATLAS Collaboration, Eur. Phys. J. C 77 (2017) 428, arXiv:1705.04176 [hep-ex].
[9] ATLAS Collaboration, arXiv:1708.03559 [hep-ex].
[10] S. Wang et al., Phys. Rev. C 44 (1991) 1091.
[11] PHENIX Collaboration, Phys. Rev. Lett. 89 (2002) 212301.
[12] ATLAS Collaboration, Phys. Rev. C 86 (2012) 014907, arXiv:1203.3087 [hep-ex].
[13] ATLAS Collaboration, Phys. Rev. Lett. 116 (2016) 172301, arXiv:1509.04776 [hep-ex].
[14] S. Cao, G.-Y. Qin and S. A. Bass, Phys. Rev. C88 (2013) 044907, arXiv: 1308.0617 [nucl-th].
[15] P. B. Gossiaux and J. Aichelin, J. Phys. G36 (2009) 064028, arXiv: 0901.2462 [nucl-th].
[16] PHENIX Collaboration, A. Adare et al., Phys. Rev. C84 (2011) 044905, arXiv: 1005.1627 [nucl-ex].
[17] ALICE Collaboration, B. Abelev et al., Phys. Rev. Lett. 111 (2013) 102301, arXiv: 1305.2707 [nucl-ex].
[18] ATLAS Collaboration, ATLAS-CONF-2015-023, 2015, url: http://cds.cern.ch/record/2055674.
[19] ATLAS Collaboration, Phys. Lett. B 707 (2012) 438, arXiv:1109.0525 [hep-ex].
[20] G. D. Moore and D. Teaney, Phys. Rev. C71 (2005) 064904, arXiv:hep-ph/0412346.
[21] N. Borghini, P. M. Dinh and J. Y. Ollitrault, Phys. Rev. C 63 (2001) 054906.
[22] A. Bilandzic, R. Snellings and S. Voloshin, Phys. Rev. C 83 (2011) 044913, arXiv: 1010.0233 [nucl-ex].
[23] ATLAS Collaboration, Eur. Phys. J. C 74 (2014) 3157, arXiv: 1408.4342 [hep-ex].
[24] ALICE Collaboration, Phys. Rev. C 90 (2014) 054901, arXiv: 1406.2474 [nucl-ex].
[25] ATLAS Collaboration, Phys. Lett. B 725 (2013) 60, arXiv: 1303.2084 [hep-ex].
[26] CMS Collaboration, Phys. Lett. B 765 (2017) 193, arXiv: 1606.06198 [nucl-ex].
[27] J. Jia, M. Zhou, and A. Trzupek, Phys. Rev. C 96 (2017) 034906, arXiv:1701.03830 [nucl-th].
[28] L. Yan and J.-Y. Ollitrault, Phys. Rev. Lett. 112 (2014) 082301, arXiv:1312.6555 [nucl-th].